



Megadroughts and pluvials in southwest Australia: 1350–2017 CE

Alison J. O'Donnell¹ · W. Lachlan McCaw² · Edward R. Cook³ · Pauline F. Grierson¹

Received: 17 November 2020 / Accepted: 19 April 2021 / Published online: 2 May 2021
© The Author(s) 2021

Abstract

Declining winter rainfall coupled with recent prolonged drought poses significant risks to water resources and agriculture across southern Australia. While rainfall declines over recent decades are largely consistent with modelled climate change scenarios, particularly for southwest Australia, the significance of these declines is yet to be assessed within the context of long-term hydroclimatic variability. Here, we present a new 668-year (1350–2017 CE) tree-ring reconstruction of autumn–winter rainfall over inland southwest Australia. This record reveals that a recent decline in rainfall over inland southwest Australia (since 2000 CE) is not unusual in terms of either magnitude or duration relative to rainfall variability over the last seven centuries. Drought periods of greater magnitude and duration than those in the instrumental record occurred prior to 1900 CE, including two ‘megadroughts’ of > 30 years duration in the eighteenth and nineteenth centuries. By contrast, the wettest > decadal periods of the last seven centuries occurred after 1900 CE, making the twentieth century the wettest of the last seven centuries. We conclude that the instrumental rainfall record (since ~ 1900 CE) does not capture the full scale of natural hydroclimatic variability for inland southwest Australia and that the risk of prolonged droughts in the region is likely much higher than currently estimated.

Keywords *Callitris* · Drought risk · Rainfall variability · Semi-arid Australia · Tree rings

1 Introduction

Prolonged droughts, rainfall declines and catastrophic floods have affected most of Australia’s major population centres and agricultural regions in recent decades, highlighting Australia’s vulnerability to extreme hydroclimatic variability (Head et al. 2014). Many of these events have been relatively well studied in terms of their impacts and potential drivers (e.g., Cai et al. 2011, 2014; van den Honert and McAneney 2011; Van Dijk et al. 2013; Ummenhofer et al. 2015). However, there is considerable uncertainty around how such events fit within the range of natural variability and how likely they are to occur, making it difficult to robustly attribute recent events to natural variability or

anthropogenic climate forcing (Cook et al. 2016; Kiem et al. 2020). Accordingly, there is an increasingly urgent need to understand the full range of natural climatic variability, particularly on decadal and longer timescales.

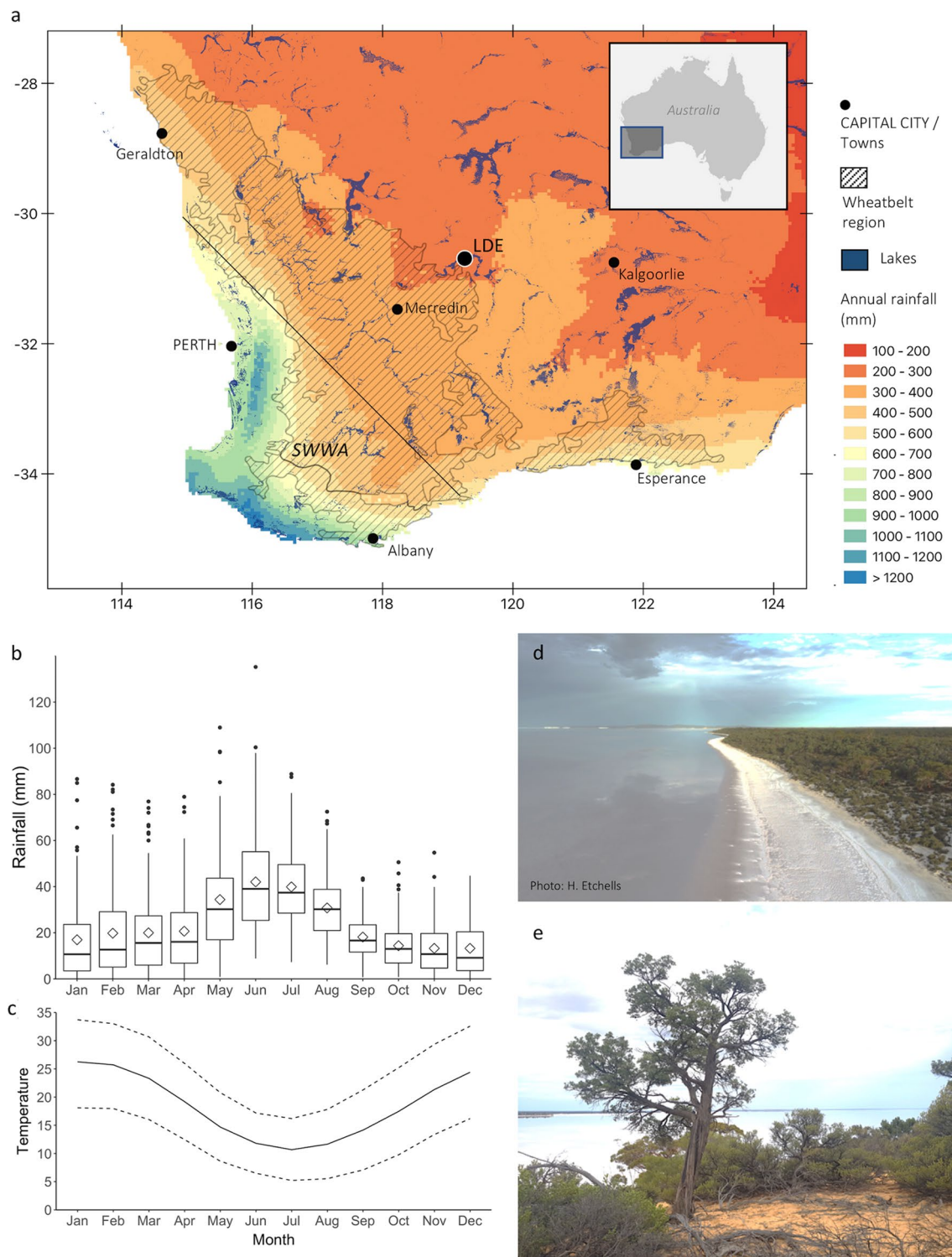
As is the case for much of the Southern Hemisphere, our ability to understand long-term climate dynamics in Australia is constrained by the short length (typically < 120 years) of instrumental climate records and the sparse spatial coverage of palaeoclimate records, particularly for mainland Australia. There are only a few high-resolution (annual), multi-century reconstructions of hydroclimate variability that are based on local proxy records from mainland Australia. These include four reconstructions based on tree-ring records (Heinrich et al. 2008; Cullen and Grierson 2009; O'Donnell et al. 2015; Allen et al. 2020) and a reconstruction based on a coral record from the Great Barrier Reef (Lough 2007, 2011). Proxy records that are remote from the Australian mainland have been used to reconstruct hydroclimate variability in eastern Australia, including tree-ring records from Indonesia, New Zealand and Tasmania (Palmer et al. 2015; Cook et al. 2016) as well as ice core records from Antarctica (e.g., Vance et al. 2013, 2015; Tozer et al. 2016; Kiem et al. 2020). However, the majority of remote records

✉ Alison J. O'Donnell
alison.odonnell@uwa.edu.au

¹ School of Biological Sciences, The University of Western Australia, Perth, WA, Australia

² Department of Biodiversity, Conservation and Attractions, Manjimup, WA, Australia

³ Lamont-Doherty Earth Observatory, Columbia University, Palisades, NY, USA



(with the exception of the Antarctic snowfall record of van Ommen and Morgan 2010) have provided little insight into hydroclimatic variability in western Australia (O'Donnell et al. 2018). This is likely in part because the dominance and impacts of remote drivers of rainfall differ between eastern and western Australia. Over eastern Australia, Pacific Ocean

circulation features including the El Niño Southern Oscillation (ENSO) and Interdecadal Pacific Oscillation (IPO) are the dominant drivers of rainfall, but these same drivers have a weaker and more variable influence on rainfall across western Australia (Risbey et al. 2009; Frederiksen et al. 2014). Instead, ocean–atmosphere circulation features

Fig. 1 Location and climate of the Lake Deborah tree-ring site in the semi-arid Mediterranean region of southwest Australia. **a** The location of the Lake Deborah (LDE) site in relation to mean annual rainfall (coloured shading) across southwest Australia and the major crop growing region of Western Australia, the Wheatbelt (hatching). The diagonal black line ($\sim 30^\circ$ S, 115° E to 35° S, 120° E) represents the approximate boundary between coastal southwest Western Australia (SWWA) and inland southwest Australia (to the northeast of the line; the focus of this study). Monthly **b** rainfall (mm) and **c** temperature ($^\circ$ C) for inland southwest Australia (CRU TS4.03 data, 1901–2017 CE, area-averaged over $29\text{--}32^\circ$ S, $117\text{--}120^\circ$ E, see Fig. 2b). **d** Photo showing the position of the tree-ring site adjacent to Lake Deborah East, a large saline ephemeral lake. **e** Photo showing an individual *Callitris columellaris* tree on white-yellow sand dune. Boxplots in **b** show the median (50th percentile) as the centre horizontal line, the interquartile range (25th to 75th percentile) as the bottom and top horizontal line, the range (0.3–99.7th percentile) as vertical lines, and extreme values (<0.7 or >99.3 percentile) of rainfall as dots. Mean monthly rainfall is indicated by diamond symbols. Lines in **c** indicate the mean monthly maximum (dotted), mean (solid) and minimum (dotted) temperatures. Rainfall data in **a** are the 1961–1990 mean annual (January to December) rainfall, available from the Australian Bureau of Meteorology (Source: http://www.bom.gov.au/jsp/ncc/climate_averages/rainfall/index.jsp). Lake data: Crossman and Li (2015) Surface Hydrology Polygons (Regional). Geoscience Australia, Canberra (<http://pid.geoscience.gov.au/dataset/ga/83134>). Wheatbelt boundary data: Vegetation—Post-European Settlement (1988). Geoscience Australia, Canberra. <http://pid.geoscience.gov.au/dataset/ga/42357>

over the Indian (i.e., the Indian Ocean Dipole, IOD) and Southern Oceans (i.e., the Southern Annular Mode), which influence rainfall in both eastern and western Australia, are more dominant as drivers of rainfall across much of western Australia than Pacific Ocean circulation features (Meneghini et al. 2007; Risbey et al. 2009).

Southwest Australia has experienced a multi-decadal decline in autumn–winter rainfall relative to the first half of the twentieth century (Indian Ocean Climate Initiative 2002; Cai and Cowan 2006; Hope et al. 2006; Timbal et al. 2006; Delworth and Zeng 2014). The observed rainfall decline has been most notable over the coastal southwest of Western Australia (SWWA), with a $\sim 20\%$ decline in autumn–winter rainfall since the 1970s (Indian Ocean Climate Initiative 2002). Since 2000 CE, the decline in rainfall across SWWA has continued and also extended further inland to encompass the main agricultural region of Western Australia (Hope and Ganter 2010; Pook et al. 2012), significantly impacting water supplies for both urban centres and agricultural regions (Bates et al. 2008; Petrone et al. 2010) as well as the profitability of agriculture (Hochman et al. 2017; Fletcher et al. 2020). However, the significance of this decline in the context of natural variability remains poorly understood.

The decline in autumn–winter rainfall over SWWA since the 1970s appears unusual in the context of instrumental records (since ~ 1900 CE) and several studies indicate that anthropogenic climate change (Cai and Cowan 2006; Hope 2006; Timbal et al. 2006; Nicholls 2010; Cai et al. 2011; Raut

et al. 2014) and possibly land clearing (Pitman et al. 2004; Timbal and Arblaster 2006; Nair et al. 2011; Andrich and Imberger 2013) have contributed to the decline. Importantly, southwest Australia is one of the few places in the world where the majority of climate models agree ($>90\%$ in both CMIP5 and CMIP6) that further declines in autumn–winter rainfall are likely in the next century with increasing anthropogenic greenhouse gas concentrations (Hope et al. 2015; Grose et al. 2020). Nevertheless, model simulations also indicate that such a decline could occur as part of natural variability on multi-decadal timescales (Cai et al. 2005). While the post-2000 CE rainfall decline over inland southwest Australia is poorly studied compared to the post-1970s decline over SWWA, a tree-ring record from the inland south of Western Australia shows that multi-decadal variability of autumn–winter rainfall has been a feature of the hydroclimate for at least 350 years (Cullen and Grierson 2009; O'Donnell et al. 2018). Additional multi-century records that are local to where rainfall declines have been observed are needed to better resolve the range of natural hydroclimatic variability across inland southwest Australia. A better understanding of the range of hydroclimatic variability is critical to more accurate assessment of the likelihood and associated risks of multi-decadal rainfall declines, prolonged ‘megadroughts’ or other extreme hydroclimatic events.

Here, we present a new annually-resolved 668-year reconstruction of autumn–winter rainfall variability for inland southwest Australia based on a local ring-width chronology of *Callitris columellaris* F. Muell. trees. This record is unique as the longest reconstruction of hydroclimate for Australia based on an Australian tree-ring record. The focus of our study is on describing the hydroclimate history of inland southwest Australia over the last seven centuries. Specifically, we aim to identify past drought and pluvial periods, including prolonged ‘mega’-droughts and pluvials (>30 years) and to interpret the significance of the recent rainfall decline in the context of climate variability of the last seven centuries. We also seek to identify whether there are coincidences of major climatic events between inland southwest Australia and other proxy records in nearby regions that may indicate teleconnections through the influence of broad-scale climate drivers. This new extended record of annually-resolved hydroclimate information is fundamental to improving understanding of the timescales of hydroclimate variability in southwest Australia and to assessing the influence of remote climate drivers in the Southern Hemisphere over the last seven centuries.

2 Site description

Our study site, referred to as Lake Deborah East (LDE), is located in inland southwest Australia at the eastern margin of the Wheatbelt region of Western Australia (30.7° S,

119.3°E, Fig. 1a). The climate of the region is considered semi-arid with an average annual rainfall of ~300 mm. The LDE site lies towards the northern limit of the “winter dominant” rainfall (Mediterranean) zone of southwest Australia. On average, most (~66%) rain in the central Wheatbelt falls during the cooler winter months (Apr–Sep), but this is highly variable from year to year (Fig. 1b, c). Autumn–winter rainfall can contribute as much as 87% or as little as 40% of annual rainfall from year to year. On average, half of autumn–winter rainfall in the region is delivered by frontal synoptic systems and approximately one third is delivered by cut-off low pressure systems, with the remainder coming from warm troughs (Pook et al. 2012). Extremes of autumn–winter rainfall can be associated with extremes of either cut off or frontal rainfall or a combination of both (Pook et al. 2012). Rainfall in the warmer summer months is typically low, but high-intensity episodic rainfall events, often associated with decaying tropical cyclones and other closed lows that track from the northwest coast of Western Australia, occur irregularly and can contribute significantly to total annual rainfall in the region (Lavender and Abbs 2013).

There are several known drivers of rainfall over inland southwest Australian, including (but not limited to) the Southern Annular Mode (SAM), the Indian Ocean Dipole (IOD) and the El Niño Southern Oscillation (ENSO), which often interact with each other to enhance or reduce the effects of each other on rainfall (see Risbey et al. 2009 for a detailed description). In particular, IOD events (positive or negative) on their own or El Niño or La Niña events on their own have a weak and variable influence on rainfall in inland southwest Australia (Risbey et al. 2009). However, when negative IOD events coincide with the La Niña phase of ENSO, their combined influence can lead to strong positive winter rainfall anomalies across southwest Australia (Risbey et al. 2009; their Fig. 7). The SAM is the leading driver of rainfall patterns in inland southwest Australia in the summer (Risbey et al. 2009; their Fig. 15). Positive SAM events in the summer months are related to wetter conditions in inland southwest Australia (Raut et al. 2014; note this is opposite to the typical influence of a positive SAM in autumn–winter in coastal southwest Western Australia, which is linked to drier conditions; Hendon et al. 2007).

Our tree-ring site is located adjacent to the shore of Lake Deborah East, one of two large, ephemeral saline lakes (the other being Lake Deborah West) that lie in the upper reaches of the Yilgarn River palaeochannel network (George et al. 2008). Our target species, the native conifer *Callitris columellaris* F.Muell. (Cupressaceae), occurs mainly on low (<10 m tall) yellow-orange sand dunes that fringe the lake. *C. columellaris* occur as scattered overstorey trees along with Salt Gum (*Eucalyptus salicola* Brooker) among a sparse shrubland of predominantly Fabaceae (mainly

Acacia) as well as Myrtaceae species (Fig. 1d, e). Several *Callitris* spp. are potentially very long-lived, but are also fire-sensitive and can only reach great ages if protected from fire (O'Donnell et al. 2010). Dry lightning storms are common in the region (Bates et al. 2015) and wildfires occur relatively frequently in the sandplain shrublands that surround the lake (O'Donnell et al. 2011). However, the LDE tree-ring site is located between two large salt lakes and surrounded by a series of smaller lakes that act as physical barriers to fire spread (O'Donnell et al. 2011). In addition, the vegetation and fuel loads at the site are sparse and unlikely to sustain the spread of fire when ignitions do occur. Consequently, some *C. columellaris* trees at LDE have been able to reach ages exceeding 500 years and the stems of some standing dead and fallen trees have remained relatively intact for at least several centuries after their death.

3 Methods

3.1 Sample collection and chronology development

We collected increment cores (5.15 mm diameter) from living trees and stem sections from dead trees (standing and fallen). Samples were prepared and crossdated using standard dendrochronological techniques (Stokes and Smiley 1968). Crossdating was quality checked using the COFECHA program (Holmes 1983; Grissino-Mayer 2001). Total ring widths were measured to the nearest 0.001 mm on a Velmex measuring stage.

Callitris columellaris trees have shallow roots and their growth is highly responsive to rainfall and soil water availability (e.g., Clayton-Greene 1981; Cullen and Grierson 2009; Brodribb et al. 2013; O'Donnell et al. 2015). *C. columellaris* are also highly drought resistant; their growth is constrained only when soil moisture content becomes extremely low (transpiration ceases when soil moisture approaches air dryness; <4%) and they can persist in a state of arrested growth for prolonged periods of drought (Clayton-Greene 1981). Intra-annual boundaries and missing rings are relatively common in *C. columellaris*, particularly in arid and semi-arid climates where rainfall is highly variable within and among years. We encountered both intra-annual and missing rings in several of the samples from the LDE site, but these were generally identified during visual inspection and crossdating. The percentage of missing rings varied among samples from <1% in most samples to ~11% in others. The percentage of intra-annual boundaries varied from ~3% to 20% among samples. It is possible that extremely dry years (drier than any observed in the instrumental period i.e., <100 mm Feb–Oct rainfall) could cause missing rings in the majority of the tree population; however, crossdating

has been used as carefully and thoroughly as possible to minimize the likelihood of this source of chronology error.

We used a signal free method (Melvin and Briffa 2008) and a time-varying response (age-dependent) spline (Melvin et al. 2007) to detrend each of the ring-width series using the RCSigFree program (<http://www.ldeo.columbia.edu/tree-ring-laboratory/resources/software>). We applied adaptive power transformations to the raw ring-width measurements prior to detrending to make them more homoscedastic (Cook and Peters 1997) and calculated ring-width indices as residuals. The final ring-width chronology included 57 series from 49 trees and showed a strong common growth signal (inter-series correlation = 0.80) and high inter-annual variability in ring width (average mean sensitivity = 0.69). The final chronology was 668 years long, covering the period between 1350 and 2017 CE (Fig. S1a).

We assessed the quality of our chronology using two parameters; the average correlation between series (RBAR) and expressed population signal (EPS) (Wigley et al. 1984; Cook and Kairiukstis 1990). RBAR provides an indication of chronology signal strength (common variance) and is independent of sample size. The EPS provides an indication of the likely loss of reconstruction accuracy as a function of RBAR and sample size, measuring how well the finite-sample chronology compares with the theoretical population chronology based on an infinite number of trees. While there is no formal level of significance for EPS, the value of 0.85 is generally accepted as a reasonable lower limit for the chronology to remain reliable. Running RBAR and EPS statistics were calculated for 51-year windows of the chronology with 25-year overlaps to assess the stability of signal strength as chronology replication diminished back in time. Both the RBAR and EPS statistics were high over the full length of the chronology (Fig. S1b), indicating that there is a strong and reliable common signal over the full 668-year (1350–2017 CE) chronology.

3.2 Rainfall data and tree growth-rainfall relationships

We obtained the Climate Research Unit's (CRU) 0.5° gridded precipitation data (TS4.03) from KNMI Climate Explorer (Trouet and van Oldenborgh 2013; <http://climexp.knmi.nl/>). We then used a combination of the *monthly_response()* function in the dendroTools package (Jevšenak and Levanič 2018) in R 3.6.1 (R Core Team 2019) and Climate Explorer to explore both temporal and spatial relationships between the ring-width chronology and rainfall in inland southwest Australia. We calculated Pearson correlation coefficients between the ring-width chronology and rainfall for each month and each period of consecutive months (between 2 and 12 months) of the current year and the previous year (24 months total) using the *monthly_response()* function.

Total rainfall over the 9-month period between February and October (Feb-Oct; Austral autumn–winter) showed the strongest correlation with tree growth ($r = 0.74$; Fig. 2a). We used Climate Explorer to examine the spatial correlation between the ring-width chronology and Feb-Oct rainfall (CRU TS4.03) across Australia. Correlations between the ring-width chronology and Feb-Oct rainfall were strong and spatially coherent across a broad area of southwest Australia (Fig. 2b). We chose an area of $3 \times 3^\circ$ around the LDE site (117° – 120° E, 29° – 32° S) where rainfall showed the strongest correlation with the ring-width chronology and then averaged the CRU TS4.03 gridded precipitation data for this area to obtain a dataset of regional rainfall as our target variable for reconstruction.

We confirmed that the $3 \times 3^\circ$ regionally-averaged CRU rainfall dataset was representative of measured rainfall in the study region by testing monthly Pearson correlations between the CRU dataset and rainfall from the instrumental weather station nearest to the LDE site (Bullfinch Station; data available for the period 1911–2017 CE from the Australian Bureau of Meteorology). The CRU and Bullfinch rainfall datasets are strongly correlated in all months, particularly in the Austral autumn and winter months (February to September; $r > 0.82$; $p < 0.0001$). Correlations between the CRU and Bullfinch datasets are still strong but slightly weaker in some of the Austral spring and summer months (October to January; $0.68 < r < 0.8$), which likely reflects that rainfall in inland southwest Australia is more episodic and spatially variable in these months and that we have averaged the CRU dataset over a relatively large ($3^\circ \times 3^\circ$) area. The CRU and Bullfinch datasets for the target season of Feb-Oct are highly correlated ($r = 0.86$; $p < 0.0001$).

3.3 Reconstruction model

We used a linear regression model to reconstruct Feb-Oct total rainfall as a function of the detrended ring-width chronology. We tested the skill of the model using the PCReg software (<http://www.ldeo.columbia.edu/tree-ring-laboratory/resources/software>) using split period calibration-verification tests that are commonly used in dendroclimatology (Fritts 1976; Cook and Kairiukstis 1990). The observed rainfall data and ring-width chronology overlapped for 117 years (1901–2017 CE). We split the data into two even periods i.e., early: 1901–1959 CE and late: 1960–2017 CE and ran two models: one using the late period as the calibration period and the early period as the verification period and the other using the early period as the calibration period and the late period as the verification period. We used two rigorous tests of fit, the reduction of error (R.E.; Fritts 1976) and the coefficient of efficiency (C.E.; Cook et al. 1999) to evaluate the skill of the models. Both models using either the early or late period for calibration pass both of these

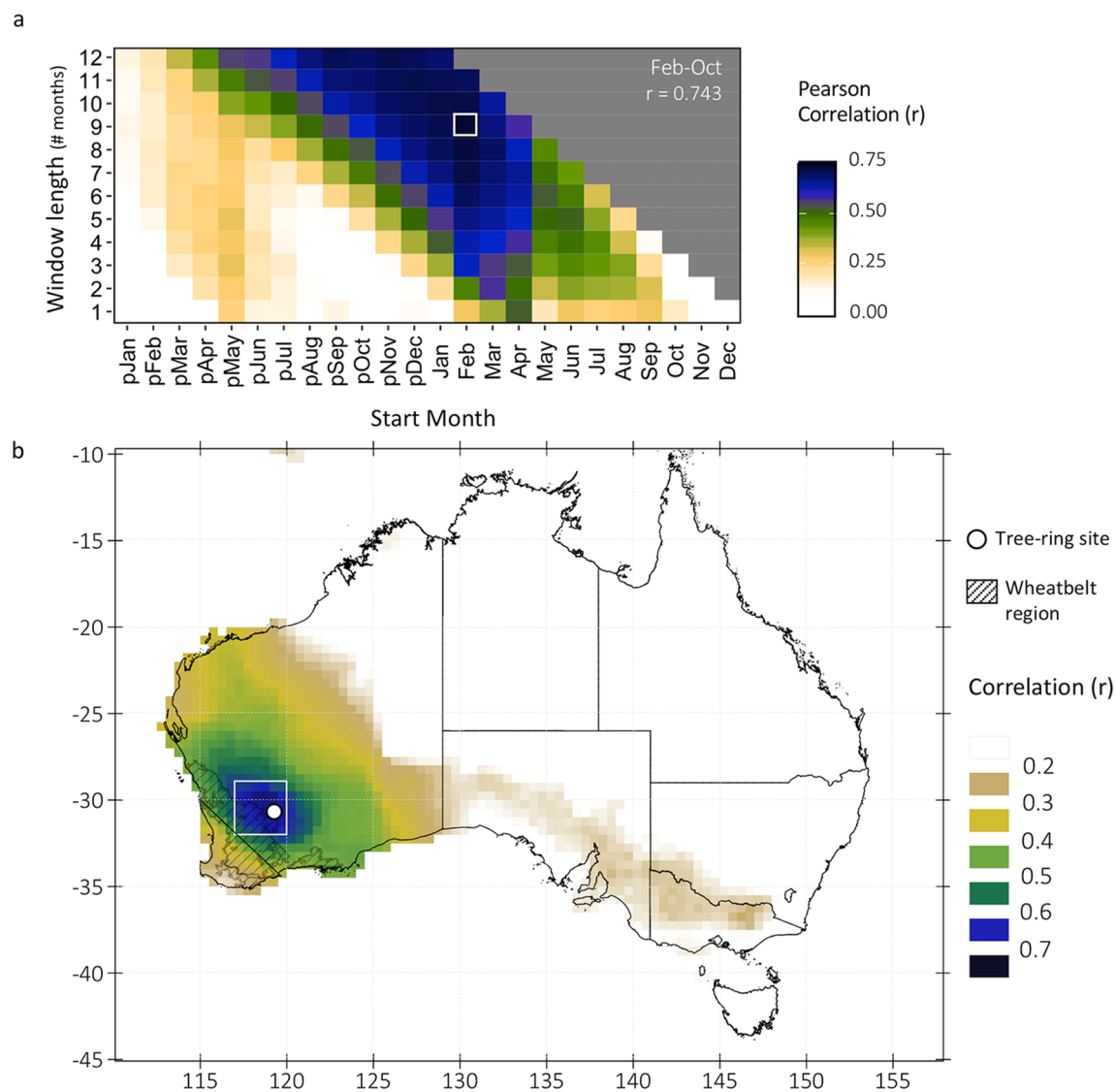


Fig. 2 Pearson correlations between the LDE chronology and **a** monthly and seasonal rainfall totals in inland southwest Australia and **b** autumn–winter (Feb–Oct total) rainfall across Australia. All rainfall data are CRU TS 4.03 0.5° gridded precipitation data, which in **a** was area-averaged over inland southwest Australia 29–32° S, 117–120° E, indicated by the white box in **(b)**. The heatmap **a** shows the correlation between the LDE chronology and rainfall summed over window lengths between 1 and 12 months (y-axis) and starting in any month of the previous (pJan–pDec) or current (Jan–Dec) year of growth (x-axis). The highest correlation was found for the 9-month window starting in February of the current year of growth (i.e., Feb–Oct

total rainfall), indicated by the white box in **(a)**. The diagonal black line (~30°S, 115°E to 35°S, 120°E) in **(b)** represents the approximate boundary between coastal southwest Western Australia (SWWA) where an autumn–winter rainfall decline has been observed since the 1970s (Indian Ocean Climate Initiative 2002) and inland southwest Australia (to the northeast of the line; the focus of this study) where an autumn–winter rainfall decline has been observed since 2000 CE. Correlations were calculated for the period 1901–2017 (i.e., $n=117$ years). Spatial correlations in **(b)** were calculated in Climate Explorer (climexp.knmi.nl)

tests ($R.E_{ver}$ and $C.E_{ver}$ are positive; Table 1) indicating that the model is skilful in reconstructing observed variation in rainfall. The linear relationship between ring width and rainfall was also stationary across the early and late calibration periods (Fig. 3a; see Wilmking et al. 2020). We then used the full period (1901–2017 CE) of observed data to develop the final linear model to reconstruct Feb–Oct total rainfall back to 1350 CE. We confirmed that there was no

significant first-order autocorrelation in the residuals of the final reconstruction model using the Durbin–Watson statistic. We then rescaled the variance of the reconstructed rainfall data to match the variance of the observed rainfall data, which allows us to make comparisons between the magnitude of events in the past and those in the observed record. The final reconstruction explains 55% of the variance of observed autumn–winter rainfall (1901–2017 CE;

Table 1 Calibration and verification statistics for the reconstruction model of autumn–winter (Feb–Oct) rainfall in inland southwest Australia

Calibration Period	r	R^2	Verification period	RE_{ver}	CE_{ver}	n
Early (1901–1959)	0.74	0.55	1960–2017	0.534	0.532	59
Late (1960–2017)	0.75	0.57	1901–1959	0.503	0.501	58
Full (1901–2017)	0.74	0.55	–	–	–	117

r is the Pearson correlation coefficient, R^2 is the coefficient of determination, RE_{ver} is the Reduction of Error and CE_{ver} is the Coefficient of Efficiency for the verification period. n is the number of data points (years) used in the model. All p -values associated with correlation values (r) are <0.0001

Fig. 3 Tests of reconstruction skill; **a** linear relationships between ring width (ring-width index) and Feb–Oct Rainfall in the early (red, 1901–1959 CE), late (blue, 1960–2017 CE) and full (black, 1901–2017 CE) calibration periods. **b** Comparison of inter-annual and multi-decadal variability (~ 40 year loess smooth) of observed rainfall (grey) and reconstructed rainfall (black) during the instrumental period (1901–2017 CE). Observed rainfall data are the CRU TS4.03 precipitation data area-averaged over 29–32° S, 117–120° E. Lines in (a) represent linear models and shaded bands represent 95% confidence intervals, calculated using the *lm()* function in R 3.6.1 (R Core Team 2019)

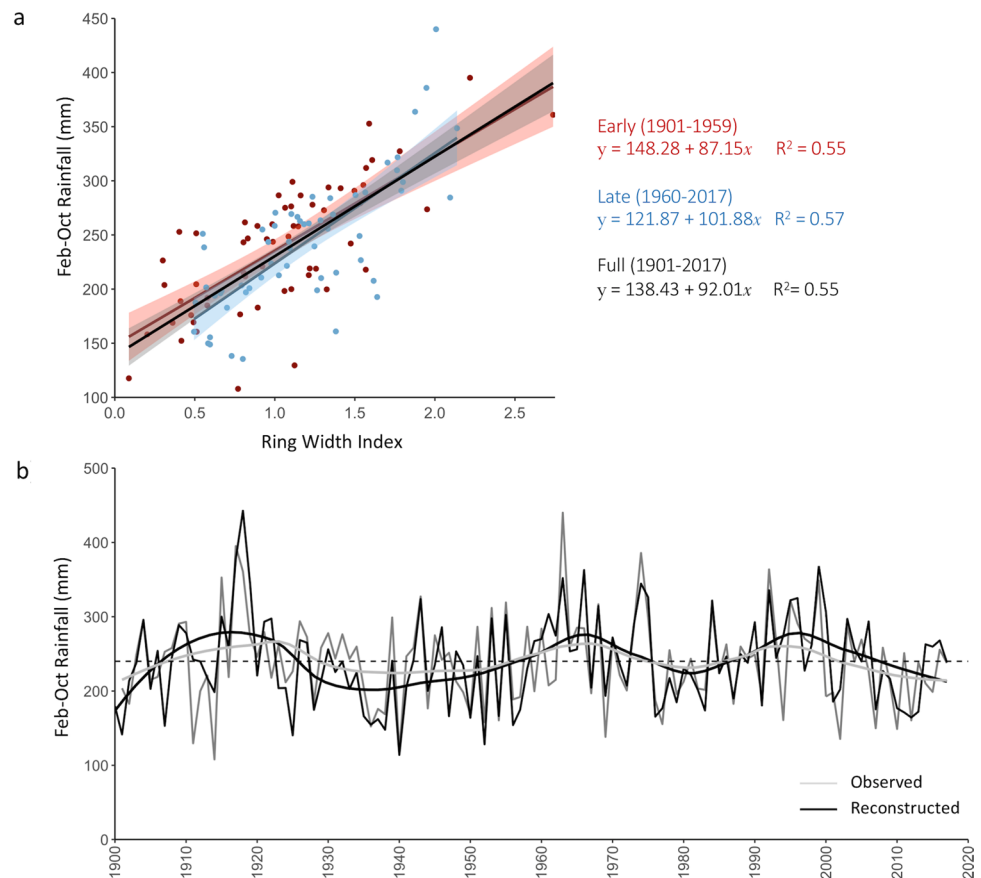


Table 1; Fig. 3a) and matches patterns of observed rainfall well on both inter-annual and decadal timescales (Fig. 3b).

Given that we were interested in interpreting the significance of the recent (post-2000 CE) observed decline in late autumn–winter (May–Oct) rainfall in inland southwest Australia, we confirmed that the reconstruction represented the observed trend well over recent decades. In particular, we considered the possibility that our tree-ring record may have been influenced by an increasing trend in summer rainfall in the post-2000 CE period (Fig S2) and thus underestimate the recent declining trend in observed autumn–winter (particularly May–Oct) rainfall. However, reconstructed rainfall represents the trend of the post-2000 CE decline in observed winter (May–Oct) rainfall well and is not strongly influenced by years of high summer rainfall in the most recent decade

(Fig S2). We consequently have confidence in using the reconstruction to assess the importance of the recent declining trend in autumn–winter rainfall in the context of rainfall variability over the last seven centuries.

3.4 Detection of ‘mega’-droughts and pluvials

We used changepoint analysis to investigate decadal and multi-decadal scale variations in hydroclimate in the reconstructed rainfall time series. Changepoint analysis is used to identify points in a time series where the statistical properties (e.g., mean, variance and/or trend) change between one period and the next (Beaulieu et al. 2012) and is often used to infer abrupt regime shifts in climate data series (e.g., Cahill et al. 2015; Rahmstorf et al. 2017). There are many

methods for detecting changepoints in timeseries data and different methods are more appropriate for some types of data or purposes than others (Rodionov 2006; Reeves et al. 2007; Liu et al. 2016; Maidstone et al. 2017; Beaulieu and Killick 2018). Here, we primarily use changepoint analysis to identify periods of above or below average rainfall and high or low inter-annual variability. We therefore used the *cpt.meanvar()* function in the changepoint package (Killick and Eckley 2014) in R 3.6.1 (R Core Team 2019) to detect changes in the mean and variance of reconstructed rainfall. We used the pruned exact linear time (PELT) method, which is an efficient and accurate method for detecting multiple changepoints in large datasets (see Killick et al. 2012), with a manually-selected penalty of $\log(n)$. We were particularly interested in identifying dry or wet periods on decadal and multi-decadal timescales as these timescales are most relevant to management of dryland agriculture and water resources. We therefore ran two analyses; one with a specified minimum segment length of 10 years (decadal), which allows for periods of any length ≥ 10 years to be identified and another with a minimum segment length of 50 years (multi-decadal). We then classified periods when mean (Feb–Oct) rainfall exceeded 0.5 standard deviations (SD) below or above the long-term (1350–2017 CE) mean of 226 mm as ‘droughts’ or ‘pluvials’. We classified periods that exceeded the 0.5 SD criterion and were > 30 years in duration as ‘megadroughts’ or ‘megapluvials’. Our focus is on the mean and variance of the identified drought and pluvial periods rather than the magnitude of the shifts that occur between them. As such, we do not intend to infer the importance of shifts between periods nor their underlying dynamics, i.e., whether the changepoints resulting from our analyses represent abrupt regime shifts rather than internal decadal or multi-decadal variability.

4 Results and discussion

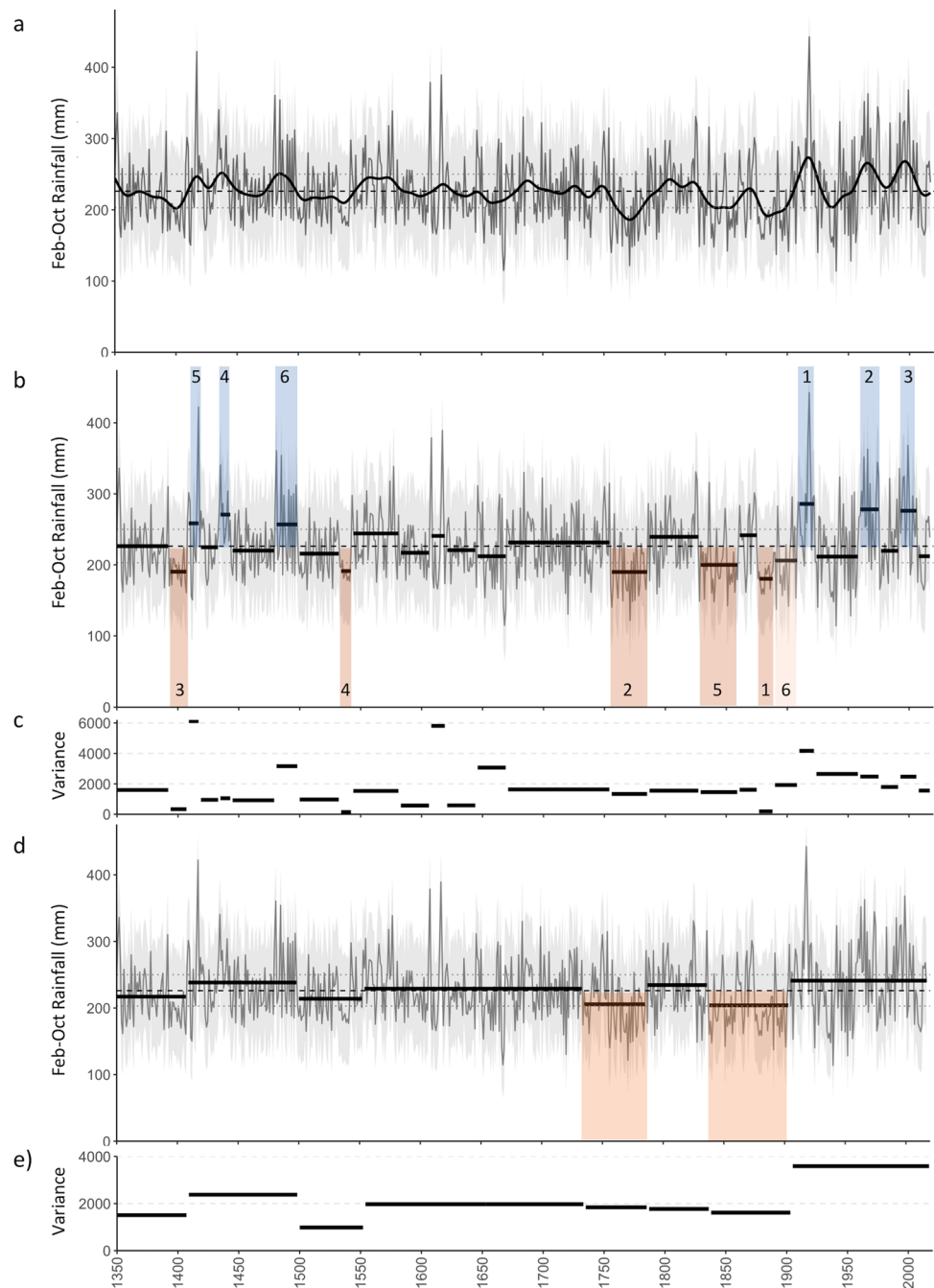
4.1 Post-2000 CE rainfall decline—is it anomalous?

Our reconstruction reveals that autumn–winter rainfall in inland southwest Australia has varied on decadal to multi-decadal timescales over the last seven centuries (Fig. 4). Our analysis also indicates that the observed autumn–winter rainfall decline over inland southwest Australia since 2000 CE is not unusual in the context of natural variability over the last seven centuries. Similar $>$ decadal declines in autumn–winter rainfall have also occurred in the fifteenth, eighteenth, nineteenth and twentieth centuries (Fig. 4a). In addition, mean rainfall for the period 2008–2017 CE was below the the 1350–2017 CE mean, but was not extremely low (~ 0.3 SD below the 1350–2017 mean; Fig. 4b).

Our tree-ring record provides empirical support for the findings of Cai et al. (2005) that multi-decadal drying trends can occur naturally over southwest Australia and suggests that natural multi-decadal scale variability could account for at least part of the rainfall decline in coastal southwest Western Australia (SWWA) and inland southwest Australia over recent decades (see Fig. 1a for the locations of SWWA and inland southwest Australia). However, these declining trends are also consistent with model-based predictions of the impact of increasing greenhouse gas concentrations on rainfall in southwest Australia (Hope 2006; Delworth and Zeng 2014; Andrys et al. 2016). In particular, the post-1970 CE rainfall decline in SWWA has been attributed to anthropogenically-driven changes in sea level pressure and the increasingly positive behaviour of the SAM over the same period, (Cai and Cowan 2006; Hope 2006; Timbal et al. 2006; Nicholls 2010; Cai et al. 2011; Raut et al. 2014) as well as changes in land cover in the region (Pitman et al. 2004; Timbal and Arblaster 2006; Nair et al. 2011; Andrich and Imberger 2013). Both natural variability and anthropogenic-driven changes likely contributed to the recent rainfall declines and their combined impacts could potentially lead to even greater reductions in rainfall in southwest Australia in the future (Cai and Cowan 2006).

While our record indicates the decline in winter rainfall over inland southwest Australia since 2000 CE is not unusual in the context of the last seven centuries, this finding does not necessarily extend to coastal SWWA, where the decline in autumn–winter rainfall has been more extreme ($> 20\%$ decline) and prolonged (since the 1970s). First, the decline in autumn–winter rainfall between 1970 and 2000 CE in SWWA was associated with a reduction in the frequency of deep low-pressure systems crossing the region (Hope et al. 2006; Hope and Ganter 2010; Raut et al. 2014). However, the continued decline post-2000 CE over SWWA and the beginning of the decline over inland southwest Australia was associated with a decline in the amount of rainfall from low-pressure systems (cutoff lows and frontal systems) rather than a further decline in their frequency, as well as an increase in the frequency of high-pressure systems, which impact a broader region of southwest Australia (Hope and Ganter 2010; Pook et al. 2012; Risbey et al. 2013). This difference in synoptic rainfall delivery systems and spatial signatures of the rainfall decline between the pre- and post-2000 CE periods suggests that different or additional drivers may be involved in the post-2000 CE decline that has impacted southwest Australia more broadly (SWWA and inland) compared to those driving the decline in only SWWA before 2000 CE (Hope and Ganter 2010). Second, an ice core record from Law Dome in Antarctica, which shows a statistically significant relationship with SWWA rainfall, suggests that the rainfall decline in SWWA since the 1970s is unusual in the context of the last seven centuries

Fig. 4 The 668-year reconstruction of autumn–winter (Feb–Oct) rainfall for inland southwest Australia showing **a** inter-annual and ~decadal variability with a ~15-year Gaussian filter; and **b, c** decadal periods (> 10 years) or **d, e** multi-decadal periods (> 50 years) identified through changepoint analysis as having different mean and variance. Horizontal solid black lines in **(b)** and **(d)** represent the mean rainfall for each period and horizontal solid black lines in **(c)** and **(e)** represent the variance of each period. Light grey shading in **(a, b, d)** represents 95% prediction intervals calculated using the *predict()* function in R 3.6.1 (R Core Team 2019); dashed horizontal black lines in **(a, b)** and **(d)** indicate mean rainfall for the full reconstruction period (1350–2017 CE); dotted horizontal lines in **(b)** and **(d)** represent $\pm 0.5SD$ from the 1350–2017 CE mean. Coloured shading in **(b)** and **(d)** indicates the driest (orange) and wettest (blue) > decadal or > multi-decadal periods in the last seven centuries. Numbers within the shaded areas in **(b)** indicate the severity rank of > decadal dry and wet periods; 1 = driest (lowest mean rainfall) or wettest (highest mean rainfall); see Table 2 for details of these periods)



(van Ommen and Morgan 2010). However, it remains uncertain whether the teleconnection between snowfall at Law Dome in Antarctica and rainfall in SWWA has been stationary through time. Hence, in situ proxy records are needed to confirm the significance of the recent rainfall decline in SWWA.

4.2 A wet twentieth century

The twentieth century was, on average, the wettest of the last seven centuries (1904–2017 CE mean rainfall ~ 15 mm

above the long-term mean; Fig. 4d) and showed a high level of inter-annual and decadal-scale variability (Fig. 4e). In particular, the twentieth century was characterised by three pluvials (with mean rainfall > 50 mm; > 1 SD above the long-term mean; Table 2; Fig. 4b). These pluvials occurred in the 1910s, 1960s–70 s and 1990s–2000s, when several strong La Niña and negative IOD events likely drove wetter conditions in inland southwest Australia (Taschetto et al. 2016; Australian Bureau of Meteorology 2020a, b). The SAM potentially also played a role in driving wet conditions during the latter half of the twentieth century. There

Table 2 The wettest and driest ≥ 10 -year periods in the last seven centuries in inland southwest Australia identified through change-point analysis

	Rank	Period	Duration (years)	Mean Rainfall (mm)	Difference from long-term mean (mm)
Wet	1	1909–1922	14	286	60
	2	1959–1975	17	278	52
	3	1992–2006	15	276	50
	4	1434–1443	10	271	45
	5	1408–1417	10	259	33
	6	1480–1498	19	257	31
Dry	1	1876–1888	13	180	-46
	2	1755–1785	31	190	-36
	3	1393–1407	15	190	-36
	4	1533–1542	10	191	-35
	5	1828–1859	32	200	-26
	6	1889–1908	20	206	-20

is a significant positive correlation between the instrumental SAM in summer-autumn (Nov–Apr, Marshall 2003) and reconstructed (Feb–Oct) rainfall in inland southwest Australia in the last half of the twentieth century ($r=0.39$, $p=0.009$, 1957–2000 CE; $r=0.41$, $p=0.006$ when both series are linearly detrended). Both instrumental and proxy records of the SAM show positive trends in the late twentieth century; which particularly between 1975 and 2000 CE, coincide with a similar positive trend in autumn–winter rainfall over inland southwest Australia (Fig S3). However, prior to the 1950s there is little agreement between our reconstruction of inland southwest Australian rainfall and proxy records of the SAM (Fig S3), suggesting that the positive relationship between the SAM and rainfall in inland southwest Australia may be a recent phenomenon. However, there is a high degree of uncertainty surrounding the behaviour of SAM prior to instrumental records. The few multi-century reconstructions of the SAM that exist (Villalba et al. 2012; Abram et al. 2014; Dätwyler et al. 2017) show little agreement with each other in the centuries prior to 1800 CE (Hessl et al. 2017; Fig S3). More SAM-sensitive records are needed to gain a more precise understanding of the temporal and geographic variability of the impacts of the SAM over the last millennium (Hessl et al. 2017) and to better characterise the relationship between the SAM and southwest Australian rainfall prior to 1950 CE.

4.3 Megadroughts in the late eighteenth and nineteenth centuries

In contrast to the twentieth century, the late eighteenth and nineteenth centuries were the driest multi-decadal periods of the last seven centuries (Fig. 4d), characterised by three

drought periods, two of which we classified as megadroughts (> 30 years duration; Fig. 4b, Table 2). The multi-decadal duration of the two megadroughts in the late eighteenth and early nineteenth centuries (#2 and #5; Fig. 4, Table 2) is of the same order as megadroughts that have been simulated for western and eastern Australia (~ 20 –40 years, Taschetto et al. 2016; Stevenson et al. 2018) and identified in an ice core-based reconstruction of eastern Australian rainfall (up to 40 years, Vance et al. 2015). Our record shows evidence of the ‘Federation drought’ at the turn of the twentieth century (1890s to 1902 CE; #6 in Fig. 4b), which is widely regarded as one of the worst droughts recorded in instrumental records in both eastern and southwest Australia (Verdon-Kidd and Kiem 2009). However, this period does not appear extreme (i.e., within 0.5 SD of the mean) in the context of the last seven centuries in inland southwest Australia. Instead, our record indicates that the decade prior (1876–1888 CE; #1 in Fig. 4b) was the most severe drought in inland southwest Australia in the last seven centuries in terms of both rainfall deficit (decadal mean) and the consistency of extremely dry conditions (i.e., absence of above average rainfall years and very low inter-annual variability; Fig. 4b, c).

There is little documented evidence from inland southwest Australia to corroborate the occurrence of megadroughts in the eighteenth and nineteenth centuries as they pre-date the development of pastoral and mining industries and thus instrumental climate records in inland southwest Australia. However, both the 1830s megadrought and the 1880s drought coincide with reports of drought conditions around Perth on the west coast of Western Australia (Foley 1957) and with dry conditions evident in a tree-ring record from the south of Western Australia (Cullen and Grierson 2009; O'Donnell et al. 2018). In addition, the 1830s was also a dry period in a tree-ring and coral based reconstruction of hydroclimate for southeast Australia (Palmer et al. 2015; Cook et al. 2016). The coincidence of drought conditions in the 1830s in southwest and southeast Australian records suggests that drought conditions may have extended across southern Australia during this period.

Interestingly, several of the drought periods evident in inland southwest Australia in the eighteenth and nineteenth centuries coincided with drought conditions evident in tree-ring based records of hydroclimate in southeast Asia. For example, the late ~ 1870 s and 1890s were also periods of severe drought conditions and famine in southeast Asia (the ‘Victorian Holocaust Droughts’ or ‘Great Drought’; Davis 2001; Buckley et al. 2007, 2019; Sano et al. 2009; Cook et al. 2010; Singh et al. 2018), which have been linked to strong El Niño conditions. In addition, the late eighteenth century megadrought (1755–1785 CE) in our record (#2 in Fig. 4b) aligns with a similar multi-decadal megadrought evident in tree-ring records from southeast Asia (‘Strange Parallels Drought’, Buckley et al. 2007, 2010; Sano et al.

2009; Cook et al. 2010). This was also a period of protracted El Niño-like conditions, as indicated by warm SST anomalies in coral records from the Galapagos Islands (Dunbar et al. 1994), suggesting that ENSO may have also played a role in driving drought conditions in both southeast Asia and southwest Australia during these periods.

4.4 Average conditions through the late sixteenth to mid-eighteenth centuries

The sixteenth to mid-eighteenth centuries appears to have been a period of relatively low multi-decadal variability of hydroclimate in inland southwest Australia (Fig. 4d). Only one drought period was identified (1540s, #4 in Fig. 4b), which, much like the 1880s drought period, was characterised by a ~decade-long run of dry years and low inter-annual variability (Fig. 4b, c). Both drought and pluvial periods were notably absent between 1550 and 1750 CE and pluvial periods in particular were absent for a ~400-year period between the sixteenth and nineteenth centuries (Fig. 4b, c).

4.5 A wet fifteenth century

The fifteenth century, much like the twentieth century, was relatively wet compared to other centuries (Fig. 4d). The fifteenth century was also characterised by three decadal pluvial periods, although these were less extreme than those in the twentieth century (mean rainfall > 30 mm or > 0.5 SD above long-term mean; Table 2; Fig. 4b, c). In general, the pluvial periods of both the fifteenth and twentieth centuries were characterised by high inter-annual variability, where extreme wet years were interspersed with dry years. However, the 1430s pluvial (#4 in Fig. 4b; Table 2) is unique among the six identified pluvial periods; characterised by a decade-long run of consistently wet conditions and low inter-annual variability (Fig. 4b, c). We identified pluvial periods with durations of up to 19 years (Table 2), but did not identify any megapluvials (> 30-year duration) in the entire 1350–2017 CE record.

The early fifteenth century was also a period of unusual climate conditions in Antarctica. Ice core records indicate periods of very low snowfall at Law Dome (east Antarctica; 1430–1470 CE; van Ommen and Morgan 2010) and low snowmelt at James Ross Island (~ 1410–1460; Abram et al. 2013) and Siple Dome (west Antarctica; Das and Alley 2008) in the early-mid 1400s, which approximately coincide with pluvial conditions in inland southwest Australia, suggesting there may have been a Southern Ocean influence linking the hydroclimate of southwest Australia and east and west Antarctica during this period. However, more independent proxy records from both southwest Australia and Antarctica would be needed to confirm this hypothesis.

4.6 Drought at the turn of the fourteenth century

We identified a drought period in inland southwest Australia between 1393 and 1407 CE (#3 in Fig. 4b; Table 2), which was characterised by a consistent run of below-average rainfall. Interestingly, this period also coincides with a severe drought period in southeast Asia (one of the ‘Angkor Droughts’) in the early fifteenth century (Buckley et al. 2010). Prolonged droughts in southeast Asia have recently been linked to low-frequency variability in Pacific Ocean climate, particularly the warm (positive) phase of the Interdecadal Pacific Oscillation (IPO; Buckley et al. 2010, 2019). While the IPO is known to influence rainfall in eastern Australia, its influence on rainfall patterns over western Australia is much more variable (Power et al. 1999; Sharmila and Hendon 2020). However, the coincidence of (mega-) droughts in both southeast Asia and southwest Australia during the fifteenth as well as late eighteenth to nineteenth centuries with positive phases of the IPO (Buckley et al. 2019), indicates that it is worth investigating the possible role of the IPO in influencing hydroclimate across the greater region during these periods.

4.7 Ongoing challenges to understanding past climate dynamics and risk

Our record covers the full period of the Little Ice Age (LIA, ~ 1400–1880 CE) but shows little evidence for a persistently dry or wet state in inland southwest Australia throughout this period; instead hydroclimate in inland southwest Australia appears to have varied between wet (fifteenth century), average (sixteenth–seventeenth centuries) and dry (late eighteenth to nineteenth centuries) states (Fig. 4). Similarly, the Australia and New Zealand Drought Atlas, a reconstruction of hydroclimate based on tree-ring and coral records that are remote from the eastern Australian mainland (Palmer et al. 2015; Cook et al. 2016) as well as a tree-ring based reconstruction of summer temperatures for Tasmania (Cook et al. 2000) do not show evidence of a persistent climate state during the LIA. In contrast, lower temporal resolution records from crater lakes in southeast Australia indicate that wet conditions were relatively persistent through the LIA, with low inter-decadal variability between ~ 1400 CE to the 1880s (Barr et al. 2014; Tibby et al. 2018), which has been attributed to La Niña-like climate forcing during the LIA (Barr et al. 2014). The lack of agreement among southern Australian proxy records during the LIA period highlights the need for greater spatial coverage and temporal resolution of proxy records to better understand the spatial and temporal patterns of past climate variability across the Australian continent.

While there have been periods of coincident climatic conditions between our record in southwest Australia and

other proxy records in the Southern Hemisphere, none of these records show consistently similar temporal patterns to ours throughout the last seven centuries. This is expected, given that rainfall in Australia is driven by complex interactions among multiple large-scale circulation features in the Indian, Southern and Pacific Oceans and that the impacts of these drivers on rainfall are often different (weaker or stronger, sometimes even opposite) in different regions of Australia (Risbey et al. 2009). However, the lack of temporally consistent relationships between our record and remote records indicates that reconstructions based on remote proxy records may not accurately represent rainfall patterns of southwest Australia. Thus, there is a need to develop more local proxy records of hydroclimate across southwest Australia and Australia more broadly to better understand rainfall variability and the temporal stability and spatial signatures of possible teleconnections with circulation features in the Pacific, Indian and Southern Oceans.

Our record indicates that decadal pluvial and drought periods have occurred irregularly in the past seven centuries; decadal droughts and pluvials primarily occurred at ~ multi-decadal frequency in several century-long periods (i.e., eighteenth century for droughts; fifteenth and twentieth centuries for pluvials), but were absent for multi-century periods in between. This finding is similar to that of Hunt (2009), who used simulated data from the CSIRO Mark 2 coupled global climatic model to estimate the occurrence of multi-year (8-year) dry periods in southwest Australia among other regions. The irregular occurrence of decadal droughts and pluvials in inland southwest Australia over the last seven centuries suggests that there is limited predictability of the occurrence of such events (Hunt 2009).

Our findings indicate that drought risk assessments need to incorporate decadal to centennial-scale variability and include the possibility of severe and prolonged droughts beyond what is currently known from the instrumental record. Our record shows that the instrumental record is restricted to the wettest period of the last seven centuries and thus under-represents prolonged and severe drought periods in inland southwest Australia, adding to growing evidence that the instrumental period (since ~ 1900 CE) does not capture the full range of rainfall variability in many regions of Australia (i.e., Vance et al. 2013; Barr et al. 2014; Allen et al. 2015; Ho et al. 2015; Cook et al. 2016; Rouillard et al. 2016; Tozer et al. 2016; Kiem et al. 2020). Hence, contemporary drought risk estimates based only on data from the instrumental period (~ 1900–present) are likely to underestimate the risk of prolonged or severe drought for this region.

Supplementary Information The online version contains supplementary material available at <https://doi.org/10.1007/s00382-021-05782-0>.

Acknowledgements This research was funded by the Australian Research Council under Discovery Grant DP170101033. We thank Douglas Ford, Hannah Etchells, and Joshua Oliver from The University of Western Australia for their assistance in collecting samples. Lamont-Doherty Earth Observatory contribution number 8501.

Author contributions All authors contributed to the study conception and design. Sample collection and preparation was performed by Alison O'Donnell, Lachlan McCaw and Pauline Grierson; data analysis was performed by Alison O'Donnell and Edward Cook. The first draft of the manuscript was written by Alison O'Donnell and all authors commented on draft versions of the manuscript. All authors read and approved the final manuscript.

Funding This research was funded by Australian Research Council Grant DP170101033.

Data availability The tree-ring width chronology and rainfall reconstruction data are available upon request from the authors and will be made freely available from the International Tree Ring Data Bank (www.ncdc.noaa.gov) upon the completion of the research project.

Declarations

Conflict of interest The authors have no conflicts of interest to declare that are relevant to the content of this article.

Ethical approval Samples were collected with permission from the Western Australian Department of Biodiversity, Conservation and Attractions under flora collection license SW019556 issued to A. O'Donnell.

Open Access This article is licensed under a Creative Commons Attribution 4.0 International License, which permits use, sharing, adaptation, distribution and reproduction in any medium or format, as long as you give appropriate credit to the original author(s) and the source, provide a link to the Creative Commons licence, and indicate if changes were made. The images or other third party material in this article are included in the article's Creative Commons licence, unless indicated otherwise in a credit line to the material. If material is not included in the article's Creative Commons licence and your intended use is not permitted by statutory regulation or exceeds the permitted use, you will need to obtain permission directly from the copyright holder. To view a copy of this licence, visit <http://creativecommons.org/licenses/by/4.0/>.

References

- Abram NJ, Mulvaney R, Wolff EW et al (2013) Acceleration of snow melt in an Antarctic Peninsula ice core during the twentieth century. *Nat Geosci* 6:404–411. <https://doi.org/10.1038/ngeo1787>
- Abram NJ, Mulvaney R, Vimeux F et al (2014) Evolution of the southern annular mode during the past millennium. *Nat Clim Change* 4:564–569. <https://doi.org/10.1038/nclimate2235>
- Allen KJ, Nichols SC, Evans R et al (2015) Preliminary December–January inflow and streamflow reconstructions from tree rings for western Tasmania, southeastern Australia. *Water Resour Res* 51:5487–5503. <https://doi.org/10.1002/2015WR017062>
- Allen KJ, Freund MB, Palmer JG et al (2020) Hydroclimate extremes in a north Australian drought reconstruction asymmetrically linked with Central Pacific Sea surface temperatures. *Glob Planet Change*. <https://doi.org/10.1016/j.gloplacha.2020.103329>

- Andrich MA, Imberger J (2013) The effect of land clearing on rainfall and fresh water resources in Western Australia: a multi-functional sustainability analysis. *Int J Sustain Dev World Ecol* 20:549–563. <https://doi.org/10.1080/13504509.2013.850752>
- Andrys J, Kala J, Lyons TJ (2016) Regional climate projections of mean and extreme climate for the southwest of Western Australia (1970–1999 compared to 2030–2059). *Clim Dyn* 1:1–25
- Australian Bureau of Meteorology (2020a) La Nina—detailed Australian analysis. <http://www.bom.gov.au/climate/enso/lnlist/>
- Australian Bureau of Meteorology (2020b) Indian Ocean Influences on Australian Climate. <http://www.bom.gov.au/climate/iod/#tabs=Indian-Ocean-climate-drivers>
- Barr C, Tibby J, Gell P et al (2014) Climate variability in south-eastern Australia over the last 1500 years inferred from the high-resolution diatom records of two crater lakes. *Quat Sci Rev* 95:115–131. <https://doi.org/10.1016/j.quascirev.2014.05.001>
- Bates BC, Hope P, Ryan B et al (2008) Key findings from the Indian Ocean Climate Initiative and their impact on policy development in Australia. *Clim Change* 89:339–354. <https://doi.org/10.1007/s10584-007-9390-9>
- Bates BC, Chandler RE, Dowdy AJ (2015) Estimating trends and seasonality in Australian monthly lightning flash counts. *J Geophys Res Atmos* 120:3973–3983. <https://doi.org/10.1002/2014JD023011>
- Beaulieu C, Killick R (2018) Distinguishing trends and shifts from memory in climate data. *J Clim* 31:9519–9543. <https://doi.org/10.1175/JCLI-D-17-0863.1>
- Beaulieu C, Chen J, Sarmiento JL (2012) Change-point analysis as a tool to detect abrupt climate variations. *Philos Trans R Soc A Math Phys Eng Sci* 370:1228–1249. <https://doi.org/10.1098/rsta.2011.0383>
- Brodribb TJ, Bowman DMJS, Grierson PF et al (2013) Conservative water management in the widespread conifer genus *Callitris*. *AoB Plants* 5:plt052–plt052. <https://doi.org/10.1093/aobpla/plt052>
- Buckley B, Palakit K, Duangsathaporn K et al (2007) Decadal scale droughts over northwestern Thailand over the past 448 years: links to the tropical Pacific and Indian Ocean sectors. *Clim Dyn* 29:63–71. <https://doi.org/10.1007/s00382-007-0225-1>
- Buckley BM, Anchukaitis KJ, Penny D et al (2010) Climate as a contributing factor in the demise of Angkor, Cambodia. *Proc Natl Acad Sci* 107:6748–6752. <https://doi.org/10.1073/pnas.0910827107>
- Buckley BM, Ummenhofer CC, D'Arrigo RD et al (2019) Interdecadal Pacific Oscillation reconstructed from trans-Pacific tree rings: 1350–2004 CE. *Clim Dyn* 53:3181–3196. <https://doi.org/10.1007/s00382-019-04694-4>
- Cahill N, Rahmstorf S, Parnell AC (2015) Change points of global temperature. *Environ Res Lett*. <https://doi.org/10.1088/1748-9326/10/8/084002>
- Cai W, Cowan T (2006) SAM and regional rainfall in IPCC AR4 models: can anthropogenic forcing account for southwest Western Australian winter rainfall reduction? *Geophys Res Lett* 33:L24708. <https://doi.org/10.1029/2006gl028037>
- Cai W, Shi G, Li Y (2005) Multidecadal fluctuations of winter rainfall over southwest Western Australia simulated in the CSIRO Mark 3 coupled model. *Geophys Res Lett* 32:1–4. <https://doi.org/10.1029/2005GL022712>
- Cai W, Van Rensch P, Borlace S, Cowan T (2011) Does the Southern Annular Mode contribute to the persistence of the multidecadal-long drought over southwest Western Australia? *Geophys Res Lett* 38:1–5. <https://doi.org/10.1029/2011GL047943>
- Cai W, Purich A, Cowan T et al (2014) Did climate change-induced rainfall trends contribute to the Australian Millennium Drought? *J Clim* 27:3145–3168. <https://doi.org/10.1175/jcli-d-13-00322.1>
- Clayton-Greene KA (1981) The autecology of *Callitris columellaris* and associated *Eucalyptus* species in south-eastern Australia. University of Melbourne, Melbourne
- Cook ER, Kairiukstis LA (1990) Methods of dendrochronology—applications. The environmental sciences. Kluwer Academic Publishers, Dordrecht
- Cook ER, Peters K (1997) Calculating unbiased tree-ring indices for the study of climatic and environmental change. *Holocene* 7:361–370. <https://doi.org/10.1177/095968369700700314>
- Cook ER, Buckley BM, D'Arrigo RD, Peterson MJ (2000) Warm-season temperatures since 1600 BC reconstructed from Tasmanian tree rings and their relationship to large-scale sea surface temperature anomalies. *Clim Dyn* 16:79–91. <https://doi.org/10.1007/s003820050006>
- Cook ER, Anchukaitis KJ, Buckley BM et al (2010) Asian monsoon failure and megadrought during the last millennium. *Science* 328:486–489. <https://doi.org/10.1126/science.1185188>
- Cook BI, Palmer JG, Cook ER et al (2016) The paleoclimate context and future trajectory of extreme summer hydroclimate in eastern Australia. *J Geophys Res Atmos* 121:12820–12838. <https://doi.org/10.1002/2016JD024892>
- Cullen LE, Grierson PF (2009) Multi-decadal scale variability in autumn–winter rainfall in south-western Australia since 1655 AD as reconstructed from tree rings of *Callitris columellaris* (Cupressaceae). *Clim Dyn* 33:433–444
- Das SB, Alley RB (2008) Rise in frequency of surface melting at Siple Dome through the Holocene: Evidence for increasing marine influence on the climate of West Antarctica. *J Geophys Res Atmos* 113:1–11. <https://doi.org/10.1029/2007JD008790>
- Dätwyler C, Neukom R, Abram NJ et al (2017) Teleconnection stationarity, variability and trends of the Southern Annular Mode (SAM) during the last millennium. *Clim Dyn*. <https://doi.org/10.1007/s00382-017-4015-0>
- Davis M (2001) Late Victorian Holocausts: El Niño Famines and the Making of the Third World. Verso, London
- Delworth TL, Zeng F (2014) Regional rainfall decline in Australia attributed to anthropogenic greenhouse gases and ozone levels. *Nat Geosci* 7:583–587. <https://doi.org/10.1038/ngeo2201>
- Dunbar RB, Wellington GM, Colgan MW, Glynn PW (1994) Eastern Pacific sea surface temperature since 1600 A.D.: The $\delta^{18}O$ record of climate variability in Galápagos Corals. *Paleoceanography* 9:291–315. <https://doi.org/10.1029/93PA03501>
- Fletcher AL, Chen C, Ota N et al (2020) Has historic climate change affected the spatial distribution of water-limited wheat yield across Western Australia? *Clim Change*. <https://doi.org/10.1007/s10584-020-02666-w>
- Foley JC (1957) Droughts in Australia: review of records from earliest years of settlement to 1955. Bureau of Meteorology, Commonwealth of Australia, Melbourne
- Frederiksen CS, Zheng X, Grainger S (2014) Teleconnections and predictive characteristics of Australian seasonal rainfall. *Clim Dyn* 43:1381–1408. <https://doi.org/10.1007/s00382-013-1952-0>
- Fritts HC (1976) Tree rings and climate. Academic Press, London
- George R, Clarke J, English P (2008) Modern and palaeogeographic trends in the salinisation of the Western Australian wheatbelt: a review. *Soil Res* 46:751. <https://doi.org/10.1071/SR080066>
- Grissino-Mayer HD (2001) Evaluating cross-dating accuracy: a manual and tutorial for the computer program COFECHA. *Tree-ring Res* 57:205–221
- Grose MR, Narsey S, Delage FP et al (2020) Insights from CMIP6 for Australia's future climate. *Earth's Future*. <https://doi.org/10.1029/2019EF001469>
- Head L, Adams M, McGregor HV, Toole S (2014) Climate change and Australia. *Wiley Interdiscip Rev Clim Chang* 5:175–197. <https://doi.org/10.1002/wcc.255>

- Heinrich I, Weidner K, Helle G et al (2008) Hydroclimatic variation in Far North Queensland since 1860 inferred from tree rings. *Palaeogeogr Palaeoclimatol Palaeoecol* 270:116–127. <https://doi.org/10.1016/j.palaeo.2008.09.002>
- Hendon HH, Thompson DWJ, Wheeler MC (2007) Australian rainfall and surface temperature variations associated with the Southern Hemisphere annular mode. *J Clim* 20:2452–2467
- Hessl A, Allen KJ, Vance T et al (2017) Reconstructions of the southern annular mode (SAM) during the last millennium. *Prog Phys Geogr* 41:834–849. <https://doi.org/10.1177/0309133317743165>
- Ho M, Kiem AS, Verdon-Kidd DC (2015) A paleoclimate rainfall reconstruction in the Murray-Darling Basin (MDB), Australia: 2. Assessing hydroclimatic risk using paleoclimate records of wet and dry epochs. *Water Resour Res* 51:8380–8396. <https://doi.org/10.1002/2015WR017059>
- Hochman Z, Gobbett DL, Horan H (2017) Climate trends account for stalled wheat yields in Australia since 1990. *Glob Chang Biol* 23:2071–2081. <https://doi.org/10.1111/gcb.13604>
- Holmes RL (1983) Computer-assisted quality control in tree-ring dating and measurement. *Tree Ring Bull* 43:111–189
- Hope PK (2006) Projected future changes in synoptic systems influencing southwest Western Australia. *Clim Dyn* 26:765–780. <https://doi.org/10.1007/s00382-006-0116-x>
- Hope P, Ganter C (2010) Recent and projected rainfall trends in South-West Australia and the associated shifts in weather systems. In: *Managing Climate Change: Papers from the Greenhouse 2009 Conference*. pp 53–63
- Hope PK, Drosowsky W, Nicholls N (2006) Shifts in the synoptic systems influencing southwest Western Australia. *Clim Dyn* 26:751–764. <https://doi.org/10.1007/s00382-006-0115-y>
- Hope P, Grose MR, Timbal B et al (2015) Seasonal and regional signature of the projected southern Australian rainfall reduction. *Aust Meteorol Oceanogr J* 65:54–71. <https://doi.org/10.22499/2.6501.005>
- Hunt BG (2009) Multi-annual dry episodes in Australian climatic variability. *Int J Climatol* 29:1715–1730. <https://doi.org/10.1002/joc.1820>
- Indian Ocean Climate Initiative (2002) Climate variability and change in south west Western Australia. Department of Environment, Water and Catchment Protection, East Perth, Western Australia, East Perth
- Jevšenak J, Levanič T (2018) dendroTools: R package for studying linear and nonlinear responses between tree-rings and daily environmental data. *Dendrochronologia* 48:32–39. <https://doi.org/10.1016/j.dendro.2018.01.005>
- Kiem AS, Vance TR, Tozer CR et al (2020) Learning from the past—using palaeoclimate data to better understand and manage drought in South East Queensland (SEQ), Australia. *J Hydrol Reg Stud* 29:100686. <https://doi.org/10.1016/j.ejrh.2020.100686>
- Killick R, Fearnhead P, Eckley IA (2012) Optimal detection of changepoints with a linear computational cost. *J Am Stat Assoc* 107:1590–1598. <https://doi.org/10.1080/01621459.2012.737745>
- Killick R, Eckley I (2014) changepoint: a comprehensive changepoint analysis package for R. *J Stat Softw*. <https://doi.org/10.18637/jss.v058.i03>
- Lavender SL, Abbs DJ (2013) Trends in Australian rainfall: contribution of tropical cyclones and closed lows. *Clim Dyn* 40:317–326. <https://doi.org/10.1007/s00382-012-1566-y>
- Liu Q, Wan S, Gu B (2016) A review of the detection methods for climate regime shifts. *Discret Dyn Nat Soc*. <https://doi.org/10.1155/2016/3536183>
- Lough JM (2007) Tropical river flow and rainfall reconstructions from coral luminescence: Great Barrier Reef, Australia. *Paleoceanography* 22:PA2218. <https://doi.org/10.1029/2006pa001377>
- Lough JM (2011) Great Barrier Reef coral luminescence reveals rainfall variability over northeastern Australia since the 17th century. *Paleoceanography* 26:PA2201. <https://doi.org/10.1029/2010pa002050>
- Maidstone R, Hocking T, Rigai G, Fearnhead P (2017) On optimal multiple changepoint algorithms for large data. *Stat Comput* 27:519–533. <https://doi.org/10.1007/s11222-016-9636-3>
- Marshall GJ (2003) Trends in the Southern Annular Mode from observations and reanalyses. *J Clim* 16:4134–4143
- Melvin TM, Briffa KR (2008) A “signal-free” approach to dendroclimatic standardisation. *Dendrochronologia* 26:71–86
- Melvin TM, Briffa KR, Nicolussi K, Grabner M (2007) Time-varying response smoothing. *Dendrochronologia* 25:65–69. <https://doi.org/10.1016/j.dendro.2007.01.004>
- Meneghini B, Simmonds I, Smith IN (2007) Association between Australian rainfall and the Southern Annular Mode. *Int J Climatol* 27:109–121. <https://doi.org/10.1002/joc.1370>
- Nair US, Wu Y, Kala J et al (2011) The role of land use change on the development and evolution of the west coast trough, convective clouds, and precipitation in southwest Australia. *J Geophys Res Atmos*. <https://doi.org/10.1029/2010JD014950>
- Nicholls N (2010) Local and remote causes of the southern Australian autumn-winter rainfall decline, 1958–2007. *Clim Dyn* 34:835–845. <https://doi.org/10.1007/s00382-009-0527-6>
- O'Donnell AJ, Cullen LE, Lachlan McCaw W et al (2010) Dendroecological potential of *Callitris preissii* for dating historical fires in semi-arid shrublands of southern Western Australia. *Dendrochronologia* 28:37–48. <https://doi.org/10.1016/j.dendro.2009.01.002>
- O'Donnell AJ, Boer MM, McCaw WL, Grierson PF (2011) Vegetation and landscape connectivity control wildfire intervals in unmanaged semi-arid shrublands and woodlands in Australia. *J Biogeogr* 38:112–124. <https://doi.org/10.1111/j.1365-2699.2010.02381.x>
- O'Donnell AJ, Cook ER, Palmer JG et al (2015) Tree rings show recent high summer-autumn precipitation in northwest Australia is unprecedented within the last two centuries. *PLoS ONE* 10:e0128533. <https://doi.org/10.1371/journal.pone.0128533>
- O'Donnell AJ, Cook ER, Palmer J et al (2018) Potential for tree rings to reveal spatial patterns of past drought variability across western Australia. *Environ Res Lett* 13:024020. <https://doi.org/10.1088/1748-9326/aaa204>
- Palmer JG, Cook ER, Turney CSM et al (2015) Drought variability in the eastern Australia and New Zealand summer drought atlas (ANZDA, CE 1500–2012) modulated by the Interdecadal Pacific Oscillation. *Environ Res Lett* 10:124002. <https://doi.org/10.1088/1748-9326/10/12/124002>
- Petrone KC, Hughes JD, Van Niel TG, Silberstein RP (2010) Streamflow decline in southwestern Australia, 1950–2008. *Geophys Res Lett* 37:1–7. <https://doi.org/10.1029/2010GL043102>
- Pitman AJ, Narisma GT, Pielke RA Sr, Holbrook NJ (2004) Impact of land cover change on the climate of southwest Western Australia. *J Geophys Res* 109:D18109. <https://doi.org/10.1029/2003jd004347>
- Pook MJ, Risbey JS, McIntosh PC (2012) The synoptic climatology of cool-season rainfall in the Central Wheatbelt of Western Australia. *Mon Weather Rev* 140:28–43. <https://doi.org/10.1175/MWR-D-11-00048.1>
- Power S, Casey T, Folland C et al (1999) Inter-decadal modulation of the impact of ENSO on Australia. *Clim Dyn* 15:319–324. <https://doi.org/10.1007/s003820050284>
- R Core Team (2019) R: a language and environment for statistical computing. R Foundation for Statistical Computing, Vienna, Austria. <http://www.R-project.org/>
- Rahmstorf S, Foster G, Cahill N (2017) Global temperature evolution: recent trends and some pitfalls. *Environ Res Lett*. <https://doi.org/10.1088/1748-9326/aa6825>

- Raut BA, Jakob C, Reeder MJ (2014) Rainfall changes over southwestern Australia and their relationship to the Southern Annular Mode and ENSO. *J Clim* 27:5801–5814. <https://doi.org/10.1175/JCLI-D-13-00773.1>
- Reeves J, Chen J, Wang XL et al (2007) A review and comparison of changepoint detection techniques for climate data. *J Appl Meteorol Climatol* 46:900–915. <https://doi.org/10.1175/JAM2493.1>
- Risbey JS, Pook MJ, McIntosh PC (2009) On the remote drivers of rainfall variability in Australia. *Mon Weather Rev* 137:3233–3253
- Risbey JS, Pook MJ, McIntosh PC (2013) Spatial trends in synoptic rainfall in southern Australia. *Geophys Res Lett* 40:3781–3785. <https://doi.org/10.1002/grl.50739>
- Rodionov SN (2006) Use of prewhitening in climate regime shift detection. *Geophys Res Lett* 33:1–4. <https://doi.org/10.1029/2006GL025904>
- Rouillard A, Skrzypek G, Turney C et al (2016) Evidence for extreme floods in arid subtropical northwest Australia during the Little Ice Age chronozone (CE 1400–1850). *Quat Sci Rev* 144:107–122. <https://doi.org/10.1016/j.quascirev.2016.05.004>
- Sano M, Buckley B, Sweda T (2009) Tree-ring based hydroclimate reconstruction over northern Vietnam from *Fokienia hodginsii*: eighteenth century mega-drought and tropical Pacific influence. *Clim Dyn* 33:331–340. <https://doi.org/10.1007/s00382-008-0454-y>
- Sharmila S, Hendon HH (2020) Mechanisms of multiyear variations of Northern Australia wet-season rainfall. *Sci Rep* 10:1–11. <https://doi.org/10.1038/s41598-020-61482-5>
- Singh D, Seager R, Cook BI et al (2018) Climate and the global famine of 1876–78. *J Clim* 31:9445–9467. <https://doi.org/10.1175/JCLI-D-18-0159.1>
- Stevenson S, Overpeck JT, Fasullo J et al (2018) Climate variability, volcanic forcing, and last millennium hydroclimate extremes. *J Clim* 31:4309–4327. <https://doi.org/10.1175/JCLI-D-17-0407.1>
- Stokes MA, Smiley TL (1968) An introduction to tree-ring dating. The University of Chicago Press, USA
- Taschetto AS, Sen GA, Ummenhofer CC, England MH (2016) Can Australian multiyear droughts and wet spells be generated in the absence of oceanic variability? *J Clim* 29:6201–6221. <https://doi.org/10.1175/JCLI-D-15-0694.1>
- Tibby J, Tyler J, Barr C (2018) Post little ice age drying of eastern Australia conflates understanding of early settlement impacts. *Quat Sci Rev*. <https://doi.org/10.1016/j.quascirev.2018.10.033>
- Timbal B, Arblaster JM (2006) Land cover change as an additional forcing to explain the rainfall decline in the south west of Australia. *Geophys Res Lett* 33:2–5. <https://doi.org/10.1029/2005GL025361>
- Timbal B, Arblaster JM, Power S (2006) Attribution of the late-twentieth-century rainfall decline in southwest Australia. *J Clim* 19:2046–2062. <https://doi.org/10.1175/JCLI3817.1>
- Tozer CR, Vance TR, Roberts JL et al (2016) An ice core derived 1013-year catchment-scale annual rainfall reconstruction in subtropical eastern Australia. *Hydrol Earth Syst Sci* 20:1703–1717. <https://doi.org/10.5194/hess-20-1703-2016>
- Trouet V, van Oldenborgh GJ (2013) KNMI Climate Explorer: a web-based research tool for high-resolution paleoclimatology. *Tree-Ring Res* 69:3–13
- Ummenhofer CC, Sen Gupta A, England MH et al (2015) How did ocean warming affect Australian rainfall extremes during the 2010/2011 *la Niña* event? *Geophys Res Lett* 42:9942–9951. <https://doi.org/10.1002/2015GL065948>
- van den Honert R, McAneney J (2011) The 2011 Brisbane floods: causes, impacts and implications. *Water* 3:1149–1173. <https://doi.org/10.3390/w3041149>
- Van Dijk AIJM, Beck HE, Crosbie RS et al (2013) The Millennium Drought in southeast Australia (2001–2009): Natural and human causes and implications for water resources, ecosystems, economy, and society. *Water Resour Res* 49:1040–1057. <https://doi.org/10.1002/wrcr.20123>
- van Ommen TD, Morgan V (2010) Snowfall increase in coastal East Antarctica linked with southwest Western Australian drought. *Nat Geosci* 3:267–272
- Vance TR, Van Ommen TD, Curran MAJ et al (2013) A millennial proxy record of ENSO and eastern Australian rainfall from the law dome ice core, east Antarctica. *J Clim* 26:710–725. <https://doi.org/10.1175/JCLI-D-12-00003.1>
- Vance TR, Roberts JL, Plummer CT et al (2015) Interdecadal Pacific variability and eastern Australian megadroughts over the last millennium. *Geophys Res Lett*. <https://doi.org/10.1002/2014GL062447>
- Verdon-Kidd DC, Kiem AS (2009) Nature and causes of protracted droughts in southeast Australia: comparison between the Federation, WWII, and big dry droughts. *Geophys Res Lett* 36:1–6. <https://doi.org/10.1029/2009GL041067>
- Villalba R, Lara A, Masiokas MH et al (2012) Unusual Southern Hemisphere tree growth patterns induced by changes in the Southern Annular Mode. *Nat Geosci* 5:793–798. <https://doi.org/10.1038/ngeo1613>
- Wigley TML, Briffa KR, Jones PD (1984) On the average value of correlated time series, with applications in dendroclimatology and hydrometeorology. *J Clim Appl Meteorol* 23:201–213
- Wilmking M, van der Maaten-Theunissen M, van der Maaten E et al (2020) Global assessment of relationships between climate and tree growth. *Glob Chang Biol* 26:3212–3220. <https://doi.org/10.1111/gcb.15057>

Publisher's Note Springer Nature remains neutral with regard to jurisdictional claims in published maps and institutional affiliations.